APL Photonics

RESEARCH ARTICLE | DECEMBER 22 2025

From ultra-noisy to ultra-stable: Optimization of the optoelectronic laser lock

Takuma Nakamura ; Yifan Liu ; Naijun Jin ; Haotian Cheng ; Charles McLemore ; Nazanin Hoghooghi ; Peter Rakich ; Franklyn Quinlan

APL Photonics 10, 126120 (2025)
https://doi.org/10.1063/5.0297890

From ultra-noisy to ultra-stable: Optimization of the optoelectronic laser lock

Cite as: APL Photon. 10, 126120 (2025); doi: 10.1063/5.0297890
Submitted: 21 August 2025 • Accepted: 9 December 2025 •
Published Online: 22 December 2025

Takuma Nakamura,[1,2,a)] Yifan Liu,[1,2] Naijun Jin,[3] Haotian Cheng,[3] Charles McLemore,[1] Nazanin Hoghooghi,[1] Peter Rakich,[3] and Franklyn Quinlan[1,4,b)]

AFFILIATIONS

[1] Time and Frequency Division, National Institute of Standards and Technology, 325 Broadway, Boulder, Colorado 80305, USA
[2] Department of Physics, University of Colorado Boulder, 440 UCB, Boulder, Colorado 80309, USA
[3] Department of Applied Physics, Yale University, New Haven, Connecticut 06520, USA
[4] Electrical, Computer and Energy Engineering, University of Colorado, Boulder, Colorado 80309, USA

[a)] **Author to whom correspondence should be addressed:** takuma.nakamura@nist.gov
[b)] franklyn.quinlan@nist.gov

ABSTRACT

We demonstrate the direct locking of a 820 kHz linewidth semiconductor distributed feedback laser to a high finesse, compact, and ultrastable reference cavity using the optoelectronic (OEO) laser locking method, resulting in cavity thermal noise-limited phase noise performance. We compare the OEO lock to the standard Pound–Drever–Hall method, demonstrating several new aspects and advantages of the OEO lock in attaining low phase noise from noisy lasers, including reducing the residual laser noise by more than 140 dB compared to its free-running level at a 10 Hz offset. In addition, we introduce a new RF feedforward noise-correction scheme that transfers the stability of the ultrastable reference cavity to an optical frequency comb even if the cavity-stabilized laser itself has high residual noise. We also reveal an OEO lock state that is capable of extremely high levels of laser noise rejection using feedforward, exceeding current theoretical models by ~15 dB. By combining compact laser sources with sub-1 ml volume and ultrastable optical cavities, this work enables extremely compact and robust ultrastable laser systems with applications in low phase noise microwave generation, sensing, and satellite ranging.

I. INTRODUCTION

Ultrastable optical frequency references are vital components in optical atomic clocks,[1] low noise microwave generation via optical frequency division,[2–4] gravitational wave detection,[5] environmental sensing,[6,7] and quantum networking,[8,9] with applications ranging from geodesy,[10] global hydrodynamics,[11] and earthquake detection[12] to microwave spectroscopy[13] and synthetic aperture radar.[14,15] To achieve the requisite level of performance, lasers need to be stabilized to a frequency reference, such as a Fabry–Pérot (FP) cavity, fiber delay line,[16] or integrated on-chip resonator.[17,18] Although many methods have been demonstrated to stabilize lasers to frequency references[19–24], Pound–Drever–Hall laser locking (PDH) has been the gold standard for more than 40 years. This is due to its numerous advantages, including robustness and a large signal-to-noise ratio, which allow for laser stabilization to less than 10^{-5} of the width of a resonance of a reference cavity, resulting in millihertz linewidth lasers.[25]

Despite its excellent track record, the PDH locking method has disadvantages, particularly for compact ultrastable laser systems. Successful locking to a high-finesse cavity typically requires a laser linewidth that is narrow to begin with. For example, kHz-level linewidths from fiber lasers, extended cavity or external-feedback diode lasers, nonplanar ring oscillator (NPRO) lasers, or otherwise pre-stabilized lasers are required to reach Hz-level laser stability.[26] With out-of-the-lab applications of ultrastable lasers moving toward compact chip-scale solutions, direct PDH locking becomes more challenging, as chip-scale lasers tend to have much larger linewidths. Furthermore, limited feedback gain at high offset frequencies results in unsuppressed residual laser noise, forming a "servo bump" in excess of the cavity noise limit. Such noise bumps are detrimental to, for example, optically derived low noise microwave signals.

As an alternative method to overcome these drawbacks, optoelectronic oscillator (OEO) laser locking offers a compelling approach. First proposed, to the best of our knowledge, in 1998 and 2000,[27,28] this method was revived in 2024 with new measurements, the addition of an optical feedforward noise correction, and new theoretical analysis.[29] In the OEO laser locking method, the laser phase noise is written onto the phase of an RF (radio frequency) carrier that oscillates in a regenerative OEO loop. The transference of the laser phase noise to the RF domain has the advantages of (1) enabling a feedback-locking servo that is proportional to phase fluctuations to provide greater noise suppression, and (2) facilitating simple-to-implement feedforward noise correction, where the phase noise of the laser is mixed with the phase noise on the OEO-generated RF carrier. In Ref. 29, this feedforward was implemented by correcting the laser phase with an acousto-optic modulator (AOM) that was driven by the OEO carrier.

In this paper, we demonstrate several new capabilities and extreme noise suppression with an OEO laser lock to a sub-1 ml volume FP resonator that make significant advances toward integrated photonics compatibility. First, we demonstrate a new feedforward correction scheme amenable to a large class of applications that rely on heterodyne detection with another optical source, such as optical frequency comb stabilization, microwave generation, or laser frequency-based sensing. With this new and simple RF feedforward noise correction scheme, we demonstrate locking of an optical frequency comb to an OEO-locked laser with high residual noise, where the resultant comb noise is nonetheless at the FP cavity thermal noise limit. We further show that careful tuning of the OEO oscillation frequency results in feedforward-corrected laser noise suppression that is 15 dB larger than current theory predicts. Finally, we show OEO laser locking can stabilize lasers with much higher noise than a PDH lock can handle, where the free-running linewidth of the laser is ~820 kHz. Feedback control of this laser results in residual laser phase noise at 10 Hz offset that is >140 dB below the free-running laser noise. We estimate this noise suppression is ~70 dB greater than is possible with PDH using the same servo electronics (although robust PDH locking was in fact not possible with this laser). Feedforward correction then further reduced the effective noise, yielding ~35 dB suppression at 1 MHz and >20 dB suppression at 5 MHz offset from the carrier frequency. By combining a compact laser source with our compact reference cavity, these results demonstrate a simple, low noise, cost-effective approach to ultrastable laser locking well-matched with many use cases of ultrastable lasers while remaining compatible with integrated photonics.

II. PRINCIPLE OF OPERATION

In this section, we briefly review the operating principle behind the OEO laser lock, and we describe how its operation allows for low noise control of optical frequency combs or other heterodyne beat signals. A schematic of the locking setup is shown in Fig. 1. Just as with a PDH lock, a continuous-wave (CW) laser is first modulated by an electro-optic phase modulator (EOM), generating discrete modulation sidebands. Unlike PDH, the modulation is created by a regenerative optoelectronic feedback loop, starting from noise. After passage through the EOM, the laser illuminates an ultrastable optical frequency reference with the laser frequency detuned from the nearest resonant optical mode. The reflection from the cavity is then directed to a photodetector. The signal from the photodetector is amplified and fed into the RF modulation port of the EOM, forming the regenerative OEO loop. Note that the frequency detuning between the laser and the cavity mode should be within the photodetector and EOM modulation bandwidth.

At the beginning of the OEO oscillation, the laser is modulated with white noise, creating broadband phase modulation of the laser. The frequency component of this modulation that is resonant with the optical cavity experiences a phase shift upon reflection, converting the original phase modulation to amplitude modulation that can be photodetected. If the detuning between the laser frequency and the cavity mode is also a resonance of the OEO loop, and the loop gain is sufficient, self-sustaining OEO oscillation occurs, creating a discrete sideband that is aligned with the mode of the optical cavity.

The OEO loop keeps the OEO modulation sideband on resonance with the optical reference cavity despite fluctuations in the optical carrier frequency. When the laser frequency shifts, if the modulation frequency is fixed, the sideband frequencies will shift commensurately. However, light stored in the optical cavity leaks out and heterodynes with the laser carrier. This shifts the frequency of the beat that defines the OEO oscillation frequency, thereby shifting the EOM modulation frequency. The adaptive shift in the EOM modulation frequency compensates for fluctuations in the laser frequency to keep the sideband on resonance with the optical cavity. The shorter the OEO loop delay, the faster the phase modulation frequency will shift to compensate. Similarly, the longer the cavity storage time, the stronger the restoring force to keep the sideband on resonance. Since the sideband stays resonant with the optical cavity, the laser phase noise (relative to the optical cavity mode) is transferred to the OEO oscillation frequency.

The transference of the laser phase noise to the OEO signal can be exploited for feedback and correction of the phase noise of the laser,[28] yielding a large reduction in the laser noise. Feedback to the laser also prevents large deviations in the laser frequency that would quench OEO oscillation. As discussed in more detail in the supplementary material, in the high gain limit, the noise reduction of this phase lock is greater than that of PDH due to the fact that, for PDH, the error signal is proportional to frequency rather than phase. As we show below, this allows for robust locking of lasers that have much higher free-running phase noise while still reaching the cavity thermal noise limit.

The fidelity by which the laser phase noise is transferred to the OEO frequency can be calculated through a linearized model (see Refs. 28 and 29 and the supplementary material). The ratio of the phase noise power spectral density (PSD) of the OEO frequency, $S_\varphi^{OEO}(f)$, to the laser phase noise PSD, $S_\varphi^{L}(f)$, is given by

$$S_\varphi^{OEO}(f)/S_\varphi^{L}(f) \approx \left(\frac{\tau_{cav}}{\tau_{cav}+\tau_{OEO}}\right)^2. \quad (1)$$

Here, τ_{OEO} is the propagation time around the OEO loop excluding the optical reference cavity, and τ_{cav} can be interpreted as the group delay of the cavity or the storage time of the optical field (twice the cavity intensity ringdown time). As τ_{cav} can exceed τ_{OEO} by several orders of magnitude, the OEO frequency gives an excellent approximation of the laser phase noise.

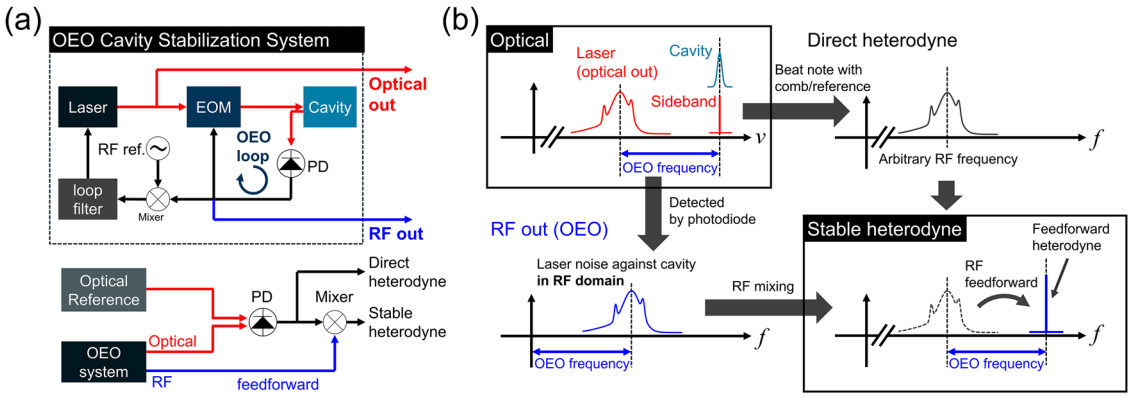

FIG. 1. (a) Schematic of the OEO laser lock (top) and RF feedforward correction (bottom). (b) Frequency domain representations of the laser, cavity mode, and resonant sideband (top left); OEO frequency (bottom left); direct heterodyne beat with an optical reference (top right); and feedforward-corrected heterodyne (bottom right).

The residual laser phase noise can be further suppressed in a simple manner with feedforward correction, particularly important at large offset frequencies where the feedback gain is reduced.[29] Feedforward correction subtracts the phase noise of the OEO loop frequency from the laser, such that the level of noise suppression with feedforward is given by

$$\left(S_\varphi^L - S_\varphi^{OEO}\right)/S_\varphi^L = \left(1 - \frac{\tau_{cav}}{\tau_{cav} + \tau_{OEO}}\right)^2 = \left(\frac{\tau_{OEO}}{\tau_{cav} + \tau_{OEO}}\right)^2 \approx \left(\frac{\tau_{OEO}}{\tau_{cav}}\right)^2. \quad (2)$$

With a τ_{cav} of a high finesse cavity as high as tens of μs and with a τ_{OEO} of tens of ns, Eq. (2) implies feedforward correction can be greater than 60 dB for large, laboratory-based cavity systems. For compact, 1 ml-volume cavities, feedforward correction can still be greater than 40 dB. Feedforward correction can be implemented by actuating on the laser with an AOM, as demonstrated in Ref. 29. However, for many important applications of cavity-stabilized lasers, such as frequency stability transfer with an optical frequency comb, feedforward does not need to be applied in the optical domain. Rather, feedforward correction can be applied to the heterodyne beat between the OEO-locked laser and the frequency comb or other laser source. Implementing this RF feedforward is performed by simply frequency-mixing the OEO oscillation frequency with the heterodyne beat. Such RF feedforward has the advantages that no additional electro-optic components are required, the OEO frequency need not match the resonant frequency of an AOM, and the correction bandwidth can be MHz wide. This is particularly advantageous when locking lasers with higher broadband noise, such as standard semiconductor lasers. It is important to note that feedforward correction is possible with PDH locking as well by taking the voltage error signal, finely tuning the voltage gain, and applying it to an electro-optic actuator.[30,31] However, feedforward with the OEO lock has the distinct benefits of a correction signal that is encoded in the phase of an RF carrier rather than a baseband voltage (such that no gain control is necessary), simple implementation with a frequency mixer, and, as shown in detail below, large noise suppression over a large bandwidth.

Finally, it is important to note that the linearized model fails to capture high-power effects, such as higher-order EOM phase modulation sidebands and the generation of harmonics of the OEO frequency, that may alter the relationship between the laser and OEO frequencies. Below, we show that, for a system appropriately tuned, the feedforward correction can be much greater than this model predicts.

III. EXPERIMENT AND RESULTS

We conducted four series of experiments on the OEO laser lock with the RF feedforward scheme and its noise suppression capacity: a comparison between PDH and OEO locking of a narrow linewidth fiber laser; optical frequency comb stabilization with RF feedforward; nonlinearity and feedforward noise suppression investigations; and OEO locking of a much larger linewidth distributed feedback (DFB) laser. For all experiments, the lasers were locked to an in-vacuum-bonded Fabry–Pérot "minicube" cavity made of ultralow expansion (ULE) glass. The cavity is manufactured with a micro-fabricated mirror and is diced out of a cavity array. In-vacuum bonding of the cavity mirrors and spacer provides a vacuum gap between the mirrors while the cavity is operated in air, resulting in thermal noise limited performance in a compact package. The cavity spacer length is 4 mm with a corresponding free-spectral range of 37.5 GHz, a finesse of about 540 000, and a full width of the resonant modes near 1550 nm of ~70 kHz (such that the resonator quality factor is ~2.7×10^9). The cavity volume is less than 1 ml, and it is placed in an air-tight enclosure measuring 50 × 50 × 30 mm^3. The cavity enclosure is not actively temperature stabilized and rests on a vibration isolation platform. More details of the cavity construction and performance may be found in Refs. 32 and 33.

A. Comparisons between OEO and PDH locking

First, we compared the phase noise performance of PDH and OEO laser locking using a narrow linewidth 1550 nm fiber laser. Locking with PDH followed the standard scheme,[34] where we utilized a 29 MHz source to sinusoidally modulate the laser phase, generating a voltage error signal that is proportional to the difference

between the laser frequency and the frequency of the FP cavity resonant mode. The error signal voltage is then conditioned by a loop filter servo with proportional, integral, and differential gain, the output of which is used to correct the laser frequency. Fast frequency corrections were performed via an AOM external to the laser, while slow, large dynamic range corrections were implemented using a piezoelectric transducer (PZT) to change the laser cavity length. For the OEO lock, the phase modulation source was replaced by the regenerative loop, as shown in Fig. 2(a). The OEO loop delay is 25 ns, determined by measuring the frequency separation between the fundamental OEO resonance and its harmonics. With this loop delay and a FP cavity half-linewidth of 35 kHz, from Eq. (2), the anticipated laser noise rejection with RF feedforward is ~45 dB. Importantly, no electrical filters are included in the OEO loop, as their inclusion can significantly increase the loop delay. The OEO loop was enclosed, although not vibration isolated. Importantly, the broad resonance of the OEO loop reduces its sensitivity to environmentally induced length fluctuations. This allows for continuous operation for days.

Any mode within the photodetector bandwidth may be chosen as the OEO oscillation frequency by appropriately detuning the laser frequency from the FP cavity mode. For the experiments reported in this section, the OEO frequency was chosen to be 85 MHz. Feedback correction to the laser was implemented by frequency-mixing the OEO frequency with an RF reference oscillator. (The RF oscillator noise should be lower than that of the reference cavity, a condition that is easily met in practice. Moreover, as shown in the supplementary material, the RF oscillator noise is greatly suppressed with our feedforward correction scheme.) The error signal from the phase locked loop then corrects the laser fluctuations using the same loop filter servo settings and feedback actuators as the PDH setup. In addition, for the fairest comparison, the optical power was kept the same between the two setups, as was the power of the RF signal applied to the EOM. In contrast to PDH, the resulting voltage error signal is proportional to the phase error of the laser.

Resulting residual and out-of-loop phase noise measurements are shown in Fig. 2(b). The out-of-loop measurements were performed by heterodyning against independent ultrastable lasers and utilizing the cross correlation measurement technique.[35] This method reveals the noise of the laser under test by rejecting the noise of the reference lasers and was particularly important for noise offset frequencies greater than ~1 kHz. For PDH, the residual, or in-loop, laser phase noise is determined by measuring the voltage noise of the error signal and calibrating against the slope of the discriminant.[36] For the OEO laser lock, the in-loop noise is the phase noise of the OEO carrier frequency when the feedback to the laser is engaged.

The free-running phase noise of the fiber laser is shown in the dotted gray curve in Fig. 2(b). To determine the free-running fiber

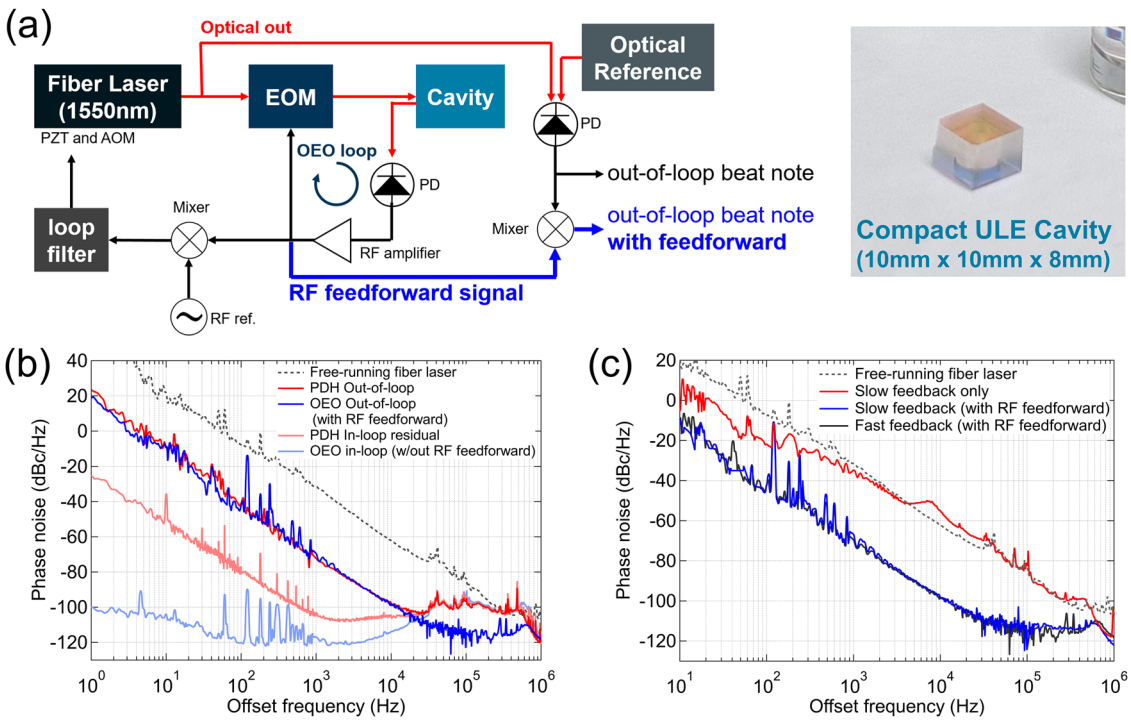

FIG. 2. (a) OEO laser lock schematic with fiber laser and minicube reference cavity. (b) Phase noise spectra with high bandwidth feedback using an AOM, comparing PDH and OEO locking with RF feedforward. Both locking methods use the same laser, loop filter, AOM for feedback control, and optical reference cavity. The OEO lock with RF feedforward follows the cavity noise limit for offset frequencies below ~100 kHz. The fiber laser's free-running noise and the in-loop residual noise of the laser for both PDH and OEO lock are shown as well. (c) Comparison of the phase noise of the fiber laser with slow, PZT-only feedback control with and without RF feedforward. With RF feedforward, the phase noise is indistinguishable from the phase noise where high bandwidth AOM feedback is used.

laser linewidth, we applied the beta separation-line method.[37] Integration of the noise to 1 Hz yielded a linewidth of 16 kHz. When locked using PDH, the phase noise of the laser output is reduced, yielding the dark red curve, and follows the cavity noise limit for offset frequencies below ~10 kHz. For larger offset frequencies, the out-of-loop noise increases above the cavity noise limit, forming a "servo bump." Comparison to the residual noise curve (light red) confirms the servo bump is a result of unsuppressed free-running laser noise due to the reduced gain in the feedback control circuit at higher offset frequencies. Note that the PDH residual noise shown here is corrected at a higher frequency offset, since the PDH error acts as a phase discriminator for offset frequencies outside the cavity linewidth. More information can be found in Ref. 38 and the supplementary material.

Exchanging the PDH circuit with the OEO laser lock with RF feedforward results in the out-of-loop phase noise shown in Fig. 2(b) in dark blue. As with PDH, the phase noise follows the cavity limit for low offset frequencies. Without feedforward correction, the noise at offset frequencies above 10 kHz would show a similar servo bump as PDH, because the feedback bandwidth is limited in the same way as PDH, as indicated by the residual OEO loop noise (light blue curve). RF feedforward correction on the heterodyne beat eliminates the servo bump, reducing the noise at 100 kHz by ~20 dB to a floor near −110 dBc/Hz. Techniques that further suppress this floor are discussed in Sec. III C. It is also interesting to compare the residual laser noise of PDH and OEO locking at low offset frequencies, where, even without feedforward correction, the OEO lock suppresses the laser noise 120 dB at 10 Hz offset, 50 dB more than PDH.

To further demonstrate the ability of feedforward correction, we increased the residual fiber laser noise by removing the AOM from the feedback circuit, leaving only the low-bandwidth PZT actuator. This greatly decreased the feedback bandwidth and increased the laser noise, as shown in the out-of-loop beat note in Fig. 2(c). Correction to the beat note with RF feedforward reduced the noise by more than 45 dB, restoring the phase noise to the cavity limit. This level of noise rejection is larger than expected from Eq. (2). Further experiments to clarify this discrepancy are described in Sec. III C.

B. Stability transfer to an optical frequency comb via RF feedforward

We demonstrate the utility of the RF feedforward by transferring thermal noise-limited cavity stability to an optical frequency comb (OFC) despite the fact that the optical signal itself can have excess noise from the source laser. Locking an OFC to a cavity-stabilized laser typically requires the formation of a heterodyne beat between the cavity-stabilized laser and a comb tooth of the OFC. This beat note is then used in a phase-lock loop to stabilize the comb to the cavity-stabilized laser. For our demonstration, we phase locked a home-built octave-spanning Er:fiber-based optical frequency comb to the OEO-locked fiber laser, the schematic of which is shown in Fig. 3(a). The OFC's offset frequency is stabilized with a conventional *f–2f* interferometer, and the comb contains an intracavity EOM for tight phase locking to optical references[4]. The fiber laser was locked to the minicube cavity with PZT feedback only, such that the laser noise again was poorly suppressed by the feedback loop. The optical frequency comb was then tightly locked to the fiber laser output via the internal EOM with and without RF feedforward. We then assessed the transfer of the cavity stability to the comb by measuring the phase noise of a beat note between another comb tooth at 1156 nm and a separate ultrastable laser that is locked to a 30 cm long FP cavity with PDH.[39]

Results are shown in Fig. 3(b). Without RF feedforward, the high residual noise of the fiber laser is transferred to the comb as expected, as shown in the red trace. On the other hand, when the RF feedforward was implemented, the phase noise of the comb at 1156 nm was greatly reduced, reaching the cavity thermal noise limit for offset frequencies below 2 kHz. Above 2 kHz offset, the

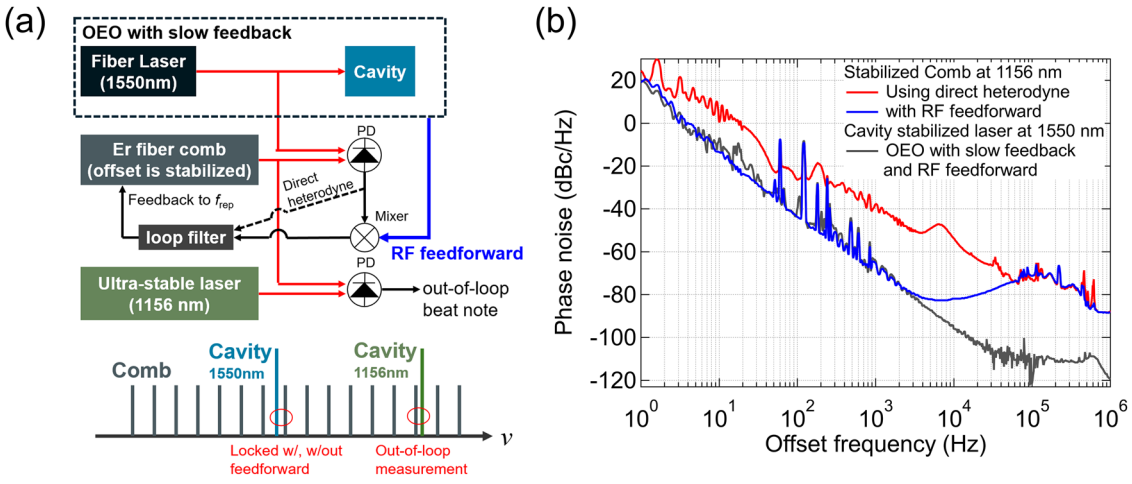

FIG. 3. Optical frequency comb locking to a cavity using the OEO laser lock. (a) Schematic (top) and frequency domain view of the optical frequency comb lock. (b) Phase noise spectra of the beat note between the frequency comb and the 1156 nm optical reference with and without the use of RF feedforward on the 1550 nm beat note between the comb and the OEO-locked laser. The phase noise of the 1550 nm laser from Fig. 2(c) is scaled to 1156 nm for comparison.

measurement is limited by noise on the 1156 nm reference laser. In addition to low noise transfer across the optical spectrum, such locking of an OFC can enable low noise microwave generation via optical frequency division while reducing the noise requirements of the free-running reference laser.[2]

C. OEO laser lock nonlinearities and enhanced laser noise suppression

While low phase noise is realized over a broad range of system parameters, we find enhanced performance can be achieved by fine-tuning the OEO lock operation. We first show distinct operation regimes as a function of the input optical power, where each regime exhibits a different OEO amplitude and phase noise level at large offset frequencies. By operating in a specific nonlinear regime, we lower the phase noise of the feedforward-corrected signal for offset frequencies >10 kHz to ~ −120 dBc/Hz. Second, we show that feedforward correction is able to suppress the laser noise beyond what is given by Eq. (2) by properly tuning the OEO oscillation frequency.

We varied the laser power to the cavity with a variable optical attenuator and identified three distinct oscillating regimes, each with unique noise properties. Results are summarized in Fig. 4. Figure 4(a) shows the OEO power driving the EOM as a function of the optical power. Once the optical power reaches the threshold needed for OEO oscillation, the OEO power increases as the optical input power is increased, denoted as region 1 in Fig. 4(a). Note that the optical powers described here to reach OEO oscillation and the reported OEO power can vary depending on the total gain of the amplifiers in the loop and V-pi of the EOM. In our case, the gain of the transimpedance amplifier following the photodiode is 10 kV/A, the RF amplifier has a gain of ~20 dB, and the EOM has a V-pi of ~3.5 V. At an optical power of 0.6 mW, the OEO power reaches a maximum of 11.4 dBm, after which it decreases with increasing optical power (region 2). At 1.4 mW of optical power, the OEO power again begins to increase (region 3). Transition from one region to the next is accompanied by a sudden change to the noise spectrum of the OEO frequency, with representative spectra shown in Fig. 4(b). Notably, the noise of region 1 is the highest and has asymmetric noise sidebands that imply correlation between the amplitude and phase noise of the OEO carrier.[40] Representative amplitude and phase noise measurements of the OEO carrier for each region of operation are shown in Fig. 4(c). The relative intensity noise (RIN) of the laser is also included in Fig. 4(c) for comparison. A noise bump near 600 kHz is common to all amplitude noise plots, the frequency of which matches the relaxation oscillation noise bump of the laser RIN. This noise peak is also present in the phase noise, implying amplitude-to-phase noise coupling, with region 2 providing the lowest noise. Thus, while feedforward correction relies on

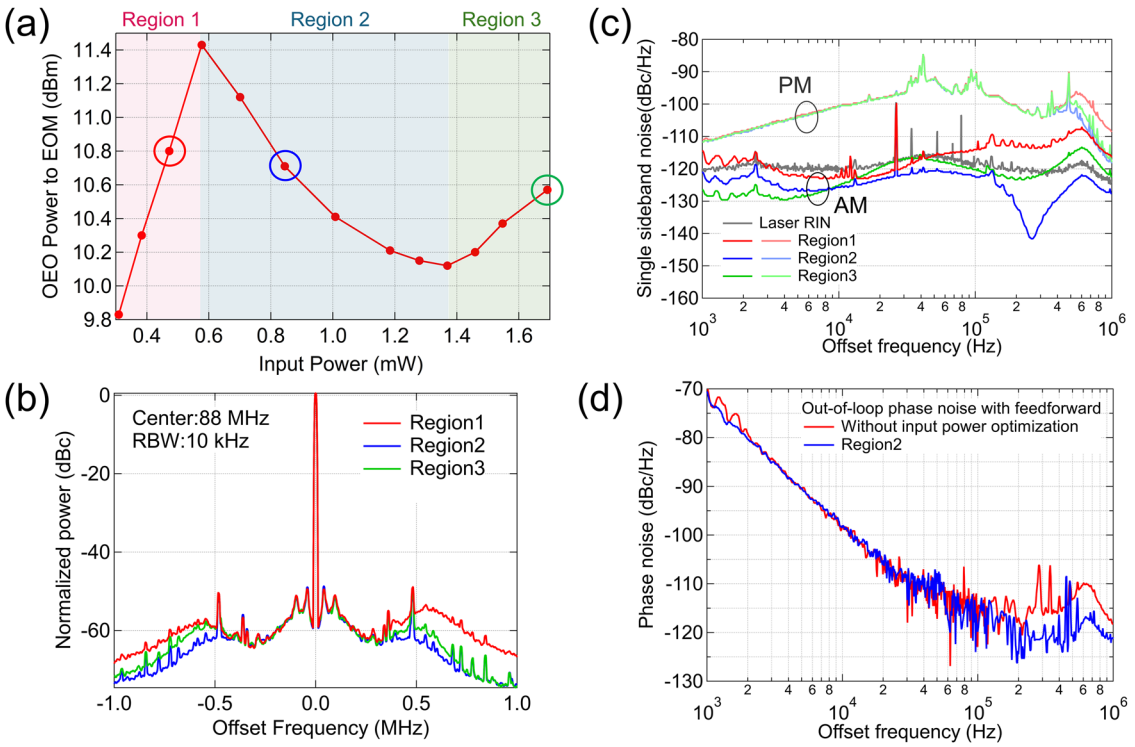

FIG. 4. (a) Measure of the OEO oscillating power as a function of optical power, where three distinct regions of operation are identified. (b) Representative spectra of the OEO frequency in the three regions of operation. Note the asymmetry of the noise sidebands, particularly for region 1; that is a hallmark of amplitude-phase noise correlation. (c) Amplitude noise (AM) and phase noise (PM) in the three operation regions. The laser RIN is shown for comparison. (d) Phase noise of the feedforward-corrected beat note without input optical power optimization compared to operation within region 2.

the OEO loop to generate a faithful copy of the laser phase noise, we believe that amplitude noise, especially at higher frequency offset, is converted to phase noise of the OEO signal. This excess OEO phase noise is not on the direct laser output, and it will not be canceled with feedforward correction. By operating in region 2, we reduce both the amplitude and the phase noise of the OEO signal, leading to lower phase noise after RF feedforward, as shown in Fig. 4(d). Noise from 100 kHz to 1 MHz is reduced 5–10 dB to ~ −120 dBc/Hz. This represents the lowest phase noise in this offset frequency range of a PDH- or OEO-locked system of which we are aware.

We employed two measurement methods to verify feedforward noise suppression beyond the predicted value of 45 dB. The first method, shown conceptually in Fig. 5(a), consisted of a 5 MHz-wide sweep of the reference synthesizer to which the OEO frequency was phase locked. This results in a sweep of the laser frequency of nearly an equal amount. Although self-sustaining OEO oscillation is centered at specific frequencies, the short OEO loop delay results in broad resonances over which the OEO frequency may be tuned.[29] Without feedforward correction, a shift in the OEO frequency results in a commensurate shift in the heterodyne beat frequency at the system output. With feedforward, however, the laser frequency shift is largely canceled, resulting in a much smaller shift of the corrected signal. Therefore, by comparing the change of the feedforward-corrected heterodyne beat to the change in the OEO frequency, the level of laser noise suppression can be estimated. As shown in Fig. 5(b), the 5 MHz OEO frequency detuning is suppressed to an average value of about 35 kHz with feedforward correction. The noise suppression ratio corresponds to around −46 dB and is consistent with the theoretical prediction. However, there is a region of near-zero slope around 0 MHz detuning, implying that the laser noise should be perfectly canceled by feedforward. To verify this, we implemented a second noise suppression measurement method. The bandwidth of the laser phase lock was reduced to less than 10 kHz, and the laser was externally frequency modulated at 20 kHz with an AOM. The phase noise power of this tone was measured with and without RF feedforward, as shown in Fig. 5(c). We measured the amount of suppression of this tone as a function of OEO frequency tuning and compared it to the slope of the frequency sweep measurement. As shown in Fig. 5(d), the agreement between these measurement techniques is excellent, not only matching the overall noise suppression level but also some of the fine structure. The noise suppression in this measurement is limited to around 60 dB, which is mainly limited by the delay error of the feedforward correction as discussed in Sec. III D and the supplementary material. While larger feedforward suppression may be achieved with fine-tuning the feedforward delay, the 20 kHz tone is already suppressed to a level very close to the measurement floor (determined by the cavity noise), such that demonstrating >60 dB suppression is

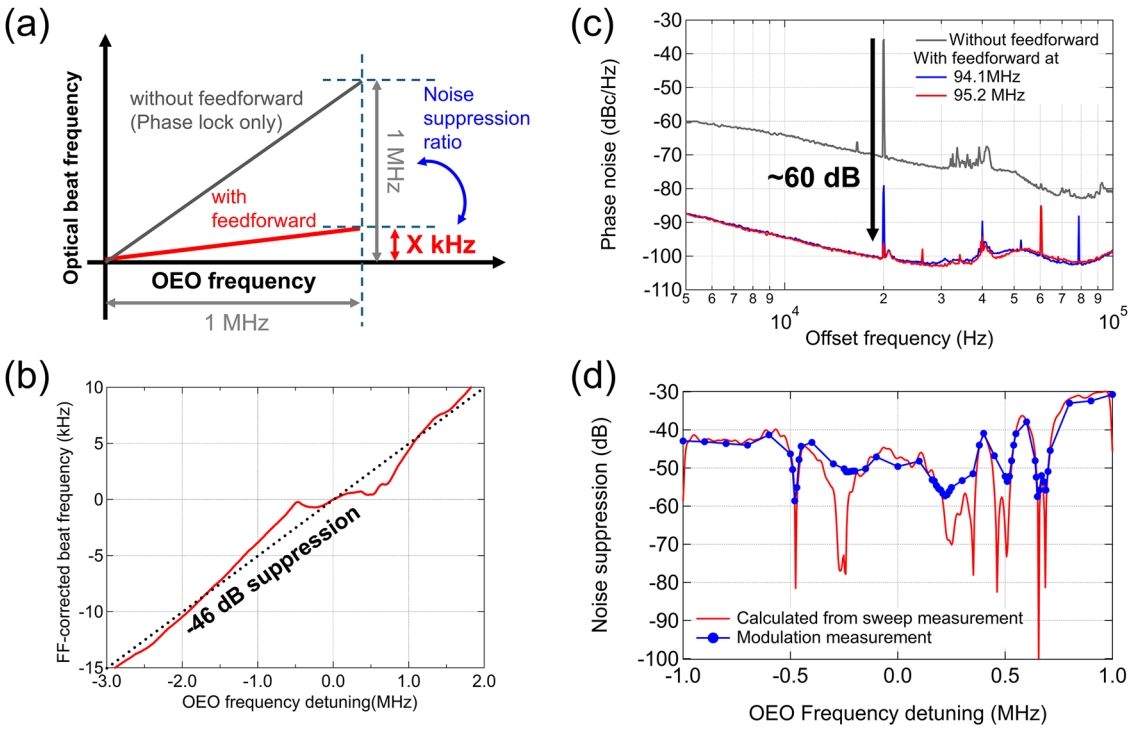

FIG. 5. Direct laser noise suppression ratio measurements. (a) OEO frequency-sweep measurement concept. (b) Measured change in the feedforward-corrected beat frequency as the OEO frequency is tuned. The dotted line indicates the slope that corresponds to 46 dB of suppression of the laser noise. Since the optical power resonant with the FP mode will vary with OEO frequency detuning, the transmitted cavity power was stabilized for this measurement. (c) Measurement of the laser phase noise suppression with RF feedforward using a discrete phase modulation tone. When the OEO oscillation frequency is 95.2 MHz, the tone is suppressed by ~60 dB, about 15 dB more than predicted by the linearized noise model. (d) Noise suppression comparison between OEO sweep and discrete tone measurements.

difficult with the current setup. Efforts to fully understand the existence of noise suppression beyond that predicted in Eq. (2) are under way. However, we find that the power in the second harmonic of the OEO oscillation frequency is correlated with regions of high noise suppression, indicating the importance of higher-order terms not included in the noise model. This is discussed further in the supplementary material.

D. DFB laser locking

The high suppression of laser noise of the OEO laser lock implies that the use of noisier chip-scale laser sources can still achieve cavity noise-limited performance. To demonstrate this, we exchanged the narrow linewidth fiber laser with a compact semiconductor DFB laser in a standard 14-pin butterfly package. The experimental schematic is shown in Fig. 6(a). The DFB laser linewidth is 820 kHz, determined by the beta-separation method from the measured phase noise, shown in the black line in Fig. 6(b). With free-running phase noise ~30 dB higher than that of the fiber laser, attempts at direct PDH locking of the DFB laser were unsuccessful. On the other hand, with the OEO locking method, the DFB laser was easily phase locked. For this, a divide-by-four frequency divider was employed, improving the lock robustness and ensuring cycle slip-free, long-term continuous operation. Importantly, frequency division for improved robustness is not an option for PDH since the frequency correction signal is directly written onto a baseband voltage. The OEO-locked DFB laser phase noise without feedforward correction is shown in the red curve of Fig. 6(b), demonstrating cavity thermal noise-limited performance for offset frequencies below ~5 kHz. Remarkably, the residual laser noise at 10 Hz offset is reduced by 140 dB from the free-running laser noise. The phase noise at offset frequencies above ~5 kHz is limited by the phase locking feedback bandwidth and gain. For applications requiring lower noise at high offset frequencies, RF feedforward greatly suppresses the residual phase noise at 10 kHz-1 MHz offset, as shown in the blue curve.

Feedforward suppresses the DFB laser noise over a much broader frequency range than is presented in the phase noise curves. Figure 6(c) shows the RF spectra of the direct heterodyne beat of the DFB laser against a separate ultrastable laser reference over a wider 10 MHz span under various operating conditions, as well as the OEO oscillation frequency. Note that the center frequencies of the various signals have been aligned in post-processing to ease comparison of the line shapes. Locking the DFB laser to the cavity greatly reduces the free-running laser linewidth (gray trace) to a coherent peak (blue trace), although noise sidebands remain. The noise of the OEO oscillating frequency (pink trace) closely matches the locked laser noise as expected, such that the noise subtraction with feedforward greatly reduces the noise of the corrected signal over a broad frequency range, shown in the red trace. The noise at 5 MHz offset

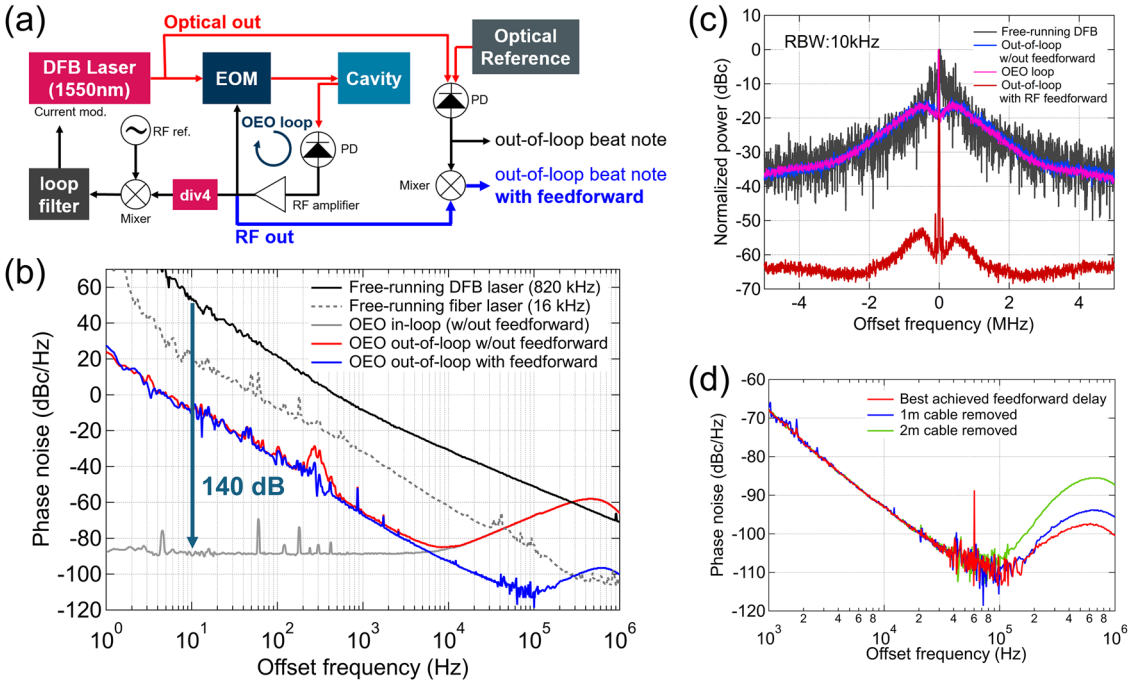

FIG. 6. OEO locking of a DFB laser to an ultrastable FP cavity. (a) Locking setup. (b) Phase noise of the locked DFB laser (blue), phase noise of the locked DFB laser with RF feedforward (red), residual laser noise of the DFB laser when locked (light gray), free-running noise of the DFB (black), and, for comparison, the free-running noise of the fiber laser from Fig. 2(b) (dotted gray). (c) Spectra of the free-running DFB laser (gray), locked DFB without feedforward correction (blue), the OEO oscillation frequency (pink), and the locked DFB with feedforward correction (red). The noise bump at ~300 Hz in the red trace is known to originate in the reference laser and not the OEO-stabilized DFB laser. (d) Phase noise of the feedforward-corrected DFB laser as a function of the delay between the heterodyne beat and the applied correction signal.

is reduced by more than 20 dB with RF feedforward, a level of suppression that is impossible with optical feedforward with an AOM, given the AOM's limited response time.

To achieve high feedforward noise suppression at high offset frequencies, the delay between the OEO frequency and the heterodyne beat must be matched correctly. As shown in Fig. 4(d), the amount of noise reduction was changed by varying the length of the RF cable used for feedforward. The best noise reduction we realized was 35 dB at 1 MHz, corresponding to a delay error of 50 cm. In this measurement, two feedforward paths are necessary for the cross correlation-based phase noise measurements. However, the length optimization was only implemented on a common feedforward line before their separation for measurement. Therefore, further length optimization for each feedforward path might further improve the phase noise. For example, to achieve 60 dB suppression at 1 MHz offset, only a 3 cm error in the cable length is acceptable. An analysis of the noise suppression limit due to delay mismatch can be found in the supplementary material.

IV. CONCLUSION

We have demonstrated OEO laser locking using a sub-1 ml, in-vacuum-bonded optical reference cavity with phase noise reaching −120 dBc/Hz at 200 kHz offset, and we introduced a new RF feedforward technique that attains broadband noise suppression, using it for low noise referencing an optical frequency comb. We have also revealed extremely high levels of laser noise rejection using feedforward that exceed current models by ~15 dB, and we have shown that robust locking of compact DFB lasers to ultrastable cavities is possible without pre-stabilization. Although not explored here, sensitivity to laser RIN, residual amplitude modulation (RAM) in the EOM, and spurious etaloning can impact the long-term stability of cavity-stabilized lasers, and a greater understanding of how these sources of frequency instability manifest in the OEO lock will be quite valuable. Considering the nonlinear behavior of the OEO lock that we have shown here, the impacts of RIN, RAM, and spurious etaloning will likely depend on the nonlinear regime of operation. We note, however, that the OEO lock has already been shown to support 10^{-15}-level fractional frequency instability.[29]

These results represent a significant advance in the capabilities of OEO laser locking, particularly relevant to out-of-the-lab applications, such as photonic microwave generation and environmental sensing, that require compact and portable ultrastable laser sources. By eliminating the requirement of a laser with low free-running noise, we anticipate that further advances of this technique will take advantage of recent developments in the combination of ultrastable reference cavities with photonic integrated circuits,[41] resulting in extremely compact and low noise laser sources. In short, the low phase noise and the system simplicity demonstrated in this paper show great potential for the OEO lock to be the next gold standard for laser stabilization.

SUPPLEMENTARY MATERIAL

See the supplementary material for theoretical analysis and further details of experiments.

ACKNOWLEDGMENTS

We thank Andrew Ludlow and the NIST Yb optical clock team for ultrastable reference light; Jun Ye and the JILA silicon cavity team for ultrastable reference light; and Dahyeon Lee, William Groman, and Tanner Grogan for their helpful comments on the paper. This work was supported by DARPA and NIST. Product names are given for scientific purposes only and do not represent an endorsement by NIST.

AUTHOR DECLARATIONS

Conflict of Interest

The authors have no conflicts to disclose.

Author Contributions

Takuma Nakamura: Conceptualization (equal); Investigation (equal); Visualization (equal); Writing – original draft (equal); Writing – review & editing (equal). **Yifan Liu**: Investigation (supporting); Writing – review & editing (supporting). **Naijun Jin**: Investigation (supporting); Writing – review & editing (supporting). **Haotian Cheng**: Investigation (supporting); Writing – review & editing (supporting). **Charles McLemore**: Investigation (supporting); Writing – review & editing (supporting). **Nazanin Hoghooghi**: Investigation (supporting); Writing – review & editing (supporting). **Peter Rakich**: Funding acquisition (equal); Supervision (equal); Writing – review & editing (supporting). **Franklyn Quinlan**: Conceptualization (equal); Funding acquisition (equal); Investigation (equal); Visualization (equal); Writing – original draft (equal); Writing – review & editing (equal).

DATA AVAILABILITY

The data that support the findings of this study are available from the corresponding author upon reasonable request.

REFERENCES

[1] A. D. Ludlow, M. M. Boyd, J. Ye, E. Peik, and P. O. Schmidt, "Optical atomic clocks," Rev. Mod. Phys. **87**, 637–701 (2015).
[2] T. M. Fortier, M. S. Kirchner, F. Quinlan, J. Taylor, J. C. Bergquist, T. Rosenband, N. Lemke, A. Ludlow, Y. Jiang, C. W. Oates, and S. a. Diddams, "Generation of ultrastable microwaves via optical frequency division," Nat. Photonics **5**, 425–429 (2011).
[3] X. Xie, R. Bouchand, D. Nicolodi, M. Giunta, W. Hänsel, M. Lezius, A. Joshi, S. Datta, C. Alexandre, M. Lours, P.-A. Tremblin, G. Santarelli, R. Holzwarth, and Y. Le Coq, "Photonic microwave signals with zeptosecond-level absolute timing noise," Nat. Photonics **11**, 44–47 (2017).
[4] T. Nakamura, J. Davila-Rodriguez, H. Leopardi, J. A. Sherman, T. M. Fortier, X. Xie, J. C. Campbell, W. F. McGrew, X. Zhang, Y. S. Hassan, D. Nicolodi, K. Beloy, A. D. Ludlow, S. A. Diddams, and F. Quinlan, "Coherent optical clock down-conversion for microwave frequencies with 10^{-18} instability," Science **368**, 889–892 (2020).
[5] R. X. Adhikari, "Gravitational radiation detection with laser interferometry," Rev. Mod. Phys. **86**, 121–151 (2014).
[6] G. Marra, D. M. Fairweather, V. Kamalov, P. Gaynor, M. Cantono, S. Mulholland, B. Baptie, J. C. Castellanos, G. Vagenas, J.-O. Gaudron, J. Kronjäger, I. R. Hill, M. Schioppo, I. Barbeito Edreira, K. A. Burrows, C. Clivati, D. Calonico, and A. Curtis, "Optical interferometry–based array of seafloor environmental sensors using a transoceanic submarine cable," Science **376**, 874–879 (2022).

[7]M. Mazur, N. K. Fontaine, M. Kelleher, V. Kamalov, R. Ryf, L. Dallachiesa, H. Chen, D. T. Neilson, and F. Quinlan, "Advanced distributed submarine cable monitoring and environmental sensing using constant power probe signals and coherent detection," arXiv:2303.06528 (2023).
[8]C. Clivati, A. Meda, S. Donadello, S. Virzì, M. Genovese, F. Levi, A. Mura, M. Pittaluga, Z. Yuan, A. J. Shields, M. Lucamarini, I. P. Degiovanni, and D. Calonico, "Coherent phase transfer for real-world twin-field quantum key distribution," Nat. Commun. **13**, 157 (2022).
[9]J.-P. Chen, C. Zhang, Y. Liu, C. Jiang, D.-F. Zhao, W.-J. Zhang, F.-X. Chen, H. Li, L.-X. You, Z. Wang, Y. Chen, X.-B. Wang, Q. Zhang, and J.-W. Pan, "Quantum key distribution over 658 km fiber with distributed vibration sensing," Phys. Rev. Lett. **128**, 180502 (2022).
[10]W. F. McGrew, X. Zhang, R. J. Fasano, S. A. Schäffer, K. Beloy, D. Nicolodi, R. C. Brown, N. Hinkley, G. Milani, M. Schioppo, T. H. Yoon, and A. D. Ludlow, "Atomic clock performance enabling geodesy below the centimetre level," Nature **564**, 87–90 (2018).
[11]F. W. Landerer, F. M. Flechtner, H. Save, F. H. Webb, T. Bandikova, W. I. Bertiger, S. V. Bettadpur, S. H. Byun, C. Dahle, H. Dobslaw, E. Fahnestock, N. Harvey, Z. Kang, G. L. H. Kruizinga, B. D. Loomis, C. McCullough, M. Murböck, P. Nagel, M. Paik, N. Pie, S. Poole, D. Strekalov, M. E. Tamisiea, F. Wang, M. M. Watkins, H. Wen, D. N. Wiese, and D. Yuan, "Extending the global mass change data record: GRACE follow-on instrument and science data performance," Geophys. Res. Lett. **47**(12), 1–10, https://doi.org/10.1029/2020GL088306 (2020).
[12]G. Marra, C. Clivati, R. Luckett, A. Tampellini, J. Kronjäger, L. Wright, A. Mura, F. Levi, S. Robinson, A. Xuereb, B. Baptie, and D. Calonico, "Ultrastable laser interferometry for earthquake detection with terrestrial and submarine cables," Science **361**, 486–490 (2018).
[13]S. Weyers, B. Lipphardt, and H. Schnatz, "Reaching the quantum limit in a fountain clock using a microwave oscillator phase locked to an ultrastable laser," Phys. Rev. A **79**, 031803 (2009).
[14]G. Krieger and M. Younis, "Impact of oscillator noise in bistatic and multistatic SAR," IEEE Geosci. Remote Sens. Lett. **3**, 424–428 (2006).
[15]K. Kellogg, P. Hoffman, S. Standley, S. Shaffer, P. Rosen, W. Edelstein, C. Dunn, C. Baker, P. Barela, Y. Shen, A. M. Guerrero, P. Xaypraseuth, V. R. Sagi, C. V Sreekantha, N. Harinath, R. Kumar, R. Bhan, and C. V. H. S. Sarma, "NASA-ISRO Synthetic Aperture Radar (NISAR) mission," in *2020 IEEE Aerospace Conference* (IEEE, 2020), pp. 1–21.
[16]I. Jeon, W. Jeong, C. Ahn, and J. Kim, "10^{-15}-level laser stabilization down to fiber thermal noise limit using self-homodyne detection," Opt. Lett. **50**, 1057 (2025).
[17]K. Liu, N. Chauhan, J. Wang, A. Isichenko, G. M. Brodnik, P. A. Morton, R. O. Behunin, S. B. Papp, and D. J. Blumenthal, "36 Hz integral linewidth laser based on a photonic integrated 4.0 m coil resonator," Optica **9**, 770 (2022).
[18]W. Loh, D. Reens, D. Kharas, A. Sumant, C. Belanger, R. T. Maxson, A. Medeiros, W. Setzer, D. Gray, K. DeBry, C. D. Bruzewicz, J. Plant, J. Liddell, G. N. West, S. Doshi, M. Roychowdhury, M. E. Kim, D. Braje, P. W. Juodawlkis, J. Chiaverini, and R. McConnell, "Optical atomic clock interrogation using an integrated spiral cavity laser," Nat. Photonics **19**, 277–283 (2025).
[19]T. W. Hansch and B. Couillaud, "Laser frequency stabilization by polarization spectroscopy of a reflecting reference cavity," Opt. Commun. **35**, 441–444 (1980).
[20]R. W. P. Drever, J. L. Hall, F. V. Kowalski, J. Hough, G. M. Ford, A. J. Munley, and H. Ward, "Laser phase and frequency stabilization using an optical resonator," Appl. Phys. B **31**, 97–105 (1983).
[21]N. M. Kondratiev, V. E. Lobanov, A. V. Cherenkov, A. S. Voloshin, N. G. Pavlov, S. Koptyaev, and M. L. Gorodetsky, "Self-injection locking of a laser diode to a high-Q WGM microresonator," Opt. Express **25**, 28167 (2017).
[22]N. Chabbra, A. R. Wade, E. Rose Rees, A. J. Sutton, A. Stochino, R. L. Ward, D. A. Shaddock, and K. McKenzie, "High stability laser locking to an optical cavity using tilt locking," Opt. Lett. **46**, 3199 (2021).
[23]F. Diorico, A. Zhutov, and O. Hosten, "Laser-cavity locking utilizing beam ellipticity: Accessing the 10^{-7} instability scale relative to cavity linewidth," Optica **11**, 26 (2024).
[24]M. H. Idjadi, K. Kim, and N. K. Fontaine, "Modulation-free laser stabilization technique using integrated cavity-coupled Mach-Zehnder interferometer," Nat. Commun. **15**, 1922 (2024).
[25]D. G. Matei, T. Legero, S. Häfner, C. Grebing, R. Weyrich, W. Zhang, L. Sonderhouse, J. M. Robinson, J. Ye, F. Riehle, and U. Sterr, "1.5 μm lasers with sub-10 mHz linewidth," Phys. Rev. Lett. **118**, 263202 (2017).
[26]A. D. Ludlow, X. Huang, M. Notcutt, T. Zanon-Willette, S. M. Foreman, M. M. Boyd, S. Blatt, and J. Ye, "Compact, thermal-noise-limited optical cavity for diode laser stabilization at 1×10^{-15}," Opt. Lett. **32**, 641 (2007).
[27]A. Wolf and H. R. Telle, "Generation of coherent optical radiation by electronic means: the electro-optical parametric oscillator," Opt. Lett. **23**, 1775 (1998).
[28]A. Wolf, B. Bodermann, and H. R. Telle, "Diode laser frequency-noise suppression by >50 dB by use of electro-optic parametric master oscillators," Opt. Lett. **25**, 1098 (2000).
[29]Q. Cen, S. Guan, D. Jiao, T. Hao, S. X. Yao, Y. Dai, and M. Li, "Ultra-narrow linewidth light generation based on an optoelectronic oscillator," arXiv:2412.02490 (2024).
[30]Y.-X. Chao, Z.-X. Hua, X.-H. Liang, Z.-P. Yue, L. You, and M. Khoon Tey, "Pound–Drever–Hall feedforward: Laser phase noise suppression beyond feedback," Optica **11**, 945 (2024).
[31]Y.-X. Chao, Z.-X. Hua, X.-H. Liang, Z.-P. Yue, C. Jia, L. You, and M. K. Tey, "Robust suppression of high-frequency laser phase noise by adaptive Pound-Drever-Hall feedforward," Phys. Rev. Appl. **23**, L011005 (2025).
[32]N. Jin, C. A. McLemore, D. Mason, J. P. Hendrie, Y. Luo, M. L. Kelleher, P. Kharel, F. Quinlan, S. A. Diddams, and P. T. Rakich, "Micro-fabricated mirrors with finesse exceeding one million," Optica **9**, 965 (2022).
[33]Y. Liu, N. Jin, D. Lee, C. McLemore, T. Nakamura, M. Kelleher, H. Cheng, S. Schima, N. Hoghooghi, S. Diddams, P. Rakich, and F. Quinlan, "Ultrastable vacuum-gap Fabry–Perot cavities operated in air," Optica **11**, 1205–1211 (2024).
[34]E. D. Black, "An introduction to Pound–Drever–Hall laser frequency stabilization," Am. J. Phys. **69**, 79–87 (2001).
[35]J. Davila-Rodriguez, F. N. Baynes, A. D. Ludlow, T. M. Fortier, H. Leopardi, S. A. Diddams, and F. Quinlan, "Compact, thermal-noise-limited reference cavity for ultra-low-noise microwave generation," Opt. Lett. **42**, 1277 (2017).
[36]T. Day, E. K. Gustafson, and R. L. Byer, "Sub-hertz relative frequency stabilization of two-diode laser-pumped Nd:YAG lasers locked to a Fabry-Perot interferometer," IEEE J. Quantum Electron. **28**, 1106–1117 (1992).
[37]G. Di Domenico, S. Schilt, and P. Thomann, "Simple approach to the relation between laser frequency noise and laser line shape," Appl. Opt. **49**, 4801 (2010).
[38]F. Bondu and O. Debieu, "Accurate measurement method of Fabry-Perot cavity parameters via optical transfer function," Appl. Opt. **46**, 2611 (2007).
[39]M. Schioppo, R. C. Brown, W. F. McGrew, N. Hinkley, R. J. Fasano, K. Beloy, T. H. Yoon, G. Milani, D. Nicolodi, J. A. Sherman, N. B. Phillips, C. W. Oates, and A. D. Ludlow, "Ultrastable optical clock with two cold-atom ensembles," Nat. Photonics **11**, 48–52 (2017).
[40]H. A. Haus and A. Mecozzi, "Noise of mode-locked lasers," IEEE J. Quantum Electron. **29**, 983–996 (1993).
[41]H. Cheng, N. Jin, Z. Dai, C. Xiang, J. Guo, Y. Zhou, S. A. Diddams, F. Quinlan, J. Bowers, O. Miller, and P. Rakich, "A novel approach to interface high-Q Fabry-Pérot resonators with photonic circuits," APL Photonics **8**, 116105 (2023).